Thermal Dependence of the Mn^{2+} and Nd^{3+} Fluorescence and of the $Mn^{2+} \rightarrow Nd^{3+}$ Energy Transfer in $RbMnF_3$

KENNETH GOOEN,* BALDASSARE DI BARTOLO,*† AND MAHBUB'UL ALAM*
MITHRAS, Division of Sanders Associates, Incorporated, Cambridge, Massachusetts 02138

AND

RICHARD C. POWELL‡
Air Force Cambridge Research Laboratories, Bedford, Massachusetts 01730

AND

ARTHUR LINZ
Department of Electrical Engineering and Center for Materials Science and Engineering, Massachusetts Institute of Technology, Cambridge, Massachusetts 02138

(Received 15 August 1968)

We have measured the absorption, excitation, and fluorescence spectra and lifetimes of Mn^{2+} and Nd^{3+} in $RbMnF_3$ in the 15–300°K region. The fluorescence spectrum of Mn^{2+} in this system presents a wide band which, going up in temperature, shows a sharp decrease in intensity and shifts its maximum from 5820 to 6300 Å at ~32°K. The Nd^{3+} emission consists of two groups of sharp lines centered at ~10 600 and 8900 Å and corresponding to the transitions ${}^4F_{3/2} \rightarrow {}^4I_{11/2}$ and ${}^4F_{3/2} \rightarrow {}^4I_{9/2}$, respectively; also, going up in temperature the intensity of the Nd^{3+} fluorescence increases sharply at ~32°K. The excitation spectra of Nd^{3+} reveal the presence of $Mn^{2+} \rightarrow Nd^{3+}$ energy transfer even at room temperature, where the Mn^{2+} fluorescence is completely quenched. The thermal variation of the Nd^{3+} fluorescence is opposite to that expected on the basis of the change in the overlapping of the Mn^{2+} fluorescence and Nd^{3+} absorption bands; this fact, together with the observed $Mn^{2+} \rightarrow Nd^{3+}$ energy transfer in the absence of the Mn^{2+} fluorescence, imply that the dominant energy-transfer mechanism is of a nonradiative type. The decay pattern of the Mn^{2+} fluorescence response in $RbMnF_3$ reveals a different behavior at ~5820 and ~6300 Å, implying the existence of two real metastable levels for Mn^{2+}. Information on the kinetics of the Mn^{2+} fluorescence and of the $Mn^{2+} \rightarrow Nd^{3+}$ energy transfer is also derived from lifetime measurements.

I. INTRODUCTION

THE object of the present investigation is twofold: (1) to study the anomalies presented by the fluorescence emission of the antiferromagnetic crystal $RbMnF_3$, and (2) to study the mechanism involved in the sensitization of the Nd^{3+} fluorescence by Mn^{2+} in $RbMnF_3$.

The fluorescence emission of $RbMnF_3$ has been studied by Holloway, Prohofsky, and Kestigian.[1,2] The fact has been recognized by them that the fluorescence spectral output of this crystal is strongly dependent on temperature, especially in the region close to $\sim\frac{1}{2}T_N$ (T_N=Neél temperature), where, going up in temperature, the peak of the fluorescence band shifts abruptly from 5820 Å to 6300 Å. Correspondingly, sudden decreases in the fluorescence intensity and lifetime are noticed. The observed anomalies are attributed by these workers to the existence of magnetic local modes strongly affected by the lattice vibrations. A cooperative effect is also postulated between the local-spin alignment and the local-lattice distortion which causes a condensation in the thermal excitation of the magnetic local mode. This picture implies the existence of one fluorescent state at each temperature, whose position, in a configurational coordinate model, is determined mainly by the degree of magnetic alignment of the excited Mn^{2+} ions.

The energy transfer mechanism from Mn^{2+} to rare-earth ions in the antiferromagnetic crystals MnF_2 and $RbMnF_3$ has been studied by Eremenko, Matyushkin, and their co-workers.[3–5] Specifically, Eremenko and co-workers studied this energy transfer in MnF_2 doped with europium by monitoring the temperature dependence of the manganese and europium fluorescence intensities. They attributed the energy transfer to a Dexter[6] type mechanism, in which the rate of the transfer is determined by the overlap of the manganese emission and the europium absorption bands.

Matyushkin and co-workers[3] studied the fluorescence decay patterns of manganese and neodymium in $RbMnF_3$ as a function of the neodymium concentration and detected the presence of Mn → Nd energy transfer and its dependence on the neodymium concentration.

* Co-sponsored by the Night Vision Laboratory, Ft. Belvoir, Va., under Contract No. DA44-009-AMC-1090(T) and by AFCRL under Contract No. F19628-68-C-0162.

† Present address: Physics Department, Boston College, Chestnut Hill, Mass.

‡ Present address: Sandia Laboratories, Albuquerque, N. M.

[1] W. W. Holloway, E. W. Prohofsky, and M. Kestigian, Phys. Rev. **139**, A954 (1965).

[2] E. W. Prohofsky, Phys. Rev. Letters **14**, 302 (1965).

[3] E. V. Matyushkin, L. S. Kukushkin, and V. V. Eremenko, Phys. Status Solidi **22**, 65 (1967).

[4] V. V. Eremenko, E. V. Matyushkin, and S. V. Petrov, Phys. Status Solidi **18**, 683 (1966).

[5] V. V. Eremenko and E. V. Matyushkin, Opt. i Spektroskopiya **23**, 437 (1967) [English transl.: Opt. Spectry. (USSR) **23**, 234 (1967)].

[6] D. L. Dexter, J. Chem. Phys. **21**, 836 (1953).

II. EXPERIMENTAL

Two samples were examined, $RbMnF_3$ and $RbMnF_3$ doped with neodymium. The dimensions of the samples were 0.8×4×5 mm and 6×5×16.5 mm, respectively.

The absorption spectra were obtained by using a Cary Model 14 recording spectrophotometer.

The fluorescence spectra were obtained by exciting the sample with a Sylvania DWY 650-W tungsten source filtered through a $CuSO_4$ solution which has a bandpass 3500–5200 Å. The fluorescence was observed at 90° to the direction of excitation, filtered through a Corning 3-69 sharp cutoff filter, chopped and focused onto the entrance slit of a Model 213 McPherson 1-m scanning monochromator which has a dispersion of ~15 Å/mm. The signal was detected by an RCA 7102 ($S-1$) photomultiplier tube cooled by liquid nitrogen, and amplified by a P.A.R. JB-5 lock-in amplifier.

The excitation measurements were performed by selectively pumping the samples by means of a Model 82-400 Jarrell-Ash monochromator and detecting the fluorescence output through proper interference filters. The resolution of the monochromator was set at about 35 Å for these measurements. A Sylvania 650-W Sun Gun was used as the exciting source.

The pulsed fluorescence measurements were made by exciting the sample with an FX-33, EG&G flash tube. The exciting radiation was filtered through a $CuSO_4$ solution. The Mn^{2+} fluorescence was passed through the McPherson monochromator with slits set at 0.5 mm; the emission was monitored at 5820 and 6300 Å and detected by a 7265 (S-20) RCA photomultiplier. The Nd^{3+} emission was passed through the 1-m monochromator set at 8720 Å with a 1-mm slit width, and detected by an RCA 7102 (S-1) photomultiplier. The fluorescence signal was observed and photographed in a Tektronix 531 oscilloscope. The time resolution of the apparatus was ~200 μsec.

For measurements at room temperature and below, the sample was mounted in a Janis Model 8DT cryostat. The sample temperature was varied by using an exchange-gas technique.

III. EXPERIMENTAL RESULTS

A. Absorption, Excitation, and Fluorescence Spectra

The absorption spectrum of $RbMnF_3:Nd^{3+}$ is shown in Fig. 1. A comparison of this spectrum with the one obtained for the undoped $RbMnF_3$ reveals that the absorption bands can be attributed to Mn^{2+}.

In Fig. 1 the bands are labeled according to Mehra and Venkateswarlu[7]; the Nd^{3+} absorption is present only in the form of some very weak absorption peaks superimposed on the Mn^{2+} bands.

We also measured the absorption spectrum of $RbMnF_3$ at ~20°K and detected the presence of sharp absorption lines superimposed on the lowest absorption band A; these lines are reported in Table I. For these measurements the absorption spectrum was observed in transmission by using the 1-m McPherson monochromator with slits set at 100 μ, corresponding to a resolution of ~1.5 Å.

We measured both the manganese and the neodymium fluorescence in $RbMnF_3:Nd^{3+}$ when illuminating the sample with light filtered through a $CuSO_4$ solution

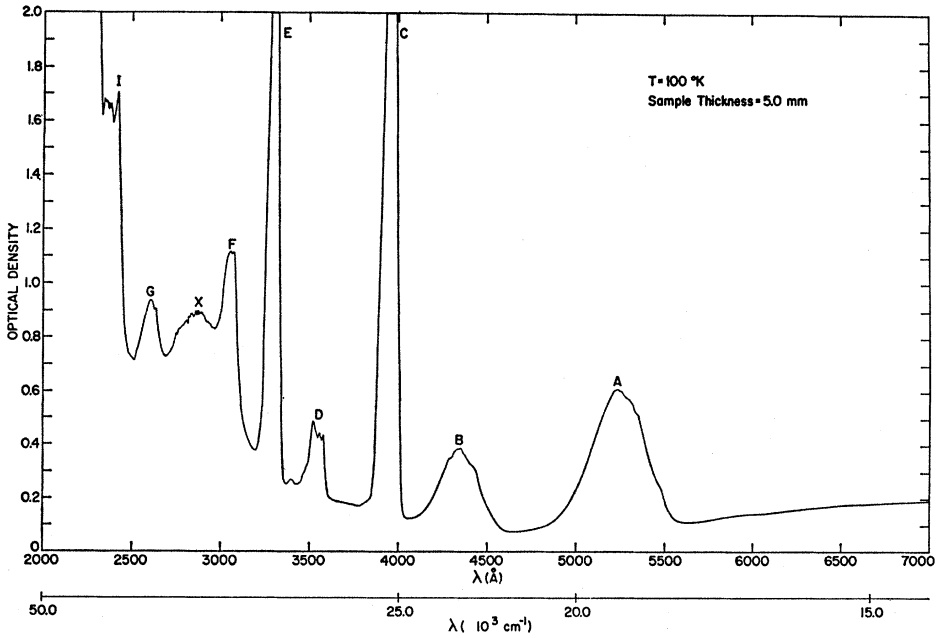

FIG. 1. Absorption spectrum of $RbMnF_3:Nd^{3+}$.

[7] A. Mehra and P. Venkateswarlu, J. Chem. Phys. 47, 2334 (1967).

and therefore pumping the systems mainly through the A, B, C, and D bands of Mn^{2+}; in the same region neodymium does not present any relevant absorption.

The fluorescence spectra of $RbMnF_3:Nd^{3+}$ are shown in Fig. 2. The fluorescence emission consists of the Nd^{3+} emission, appearing as two groups of sharp lines centered at 10 500 and 8900 Å and of a prominent manganese band.

The variations of the position and intensity of the manganese emission are the same as those observed in the undoped $RbMnF_3$ sample and are reported in more detail in Fig. 3. The band is ~500 Å wide and centered at 5820 Å at 25°K. Going up in temperature, the fluorescence band shifts its peak abruptly to 6300 Å at ~32°K and decreases in intensity at the same time. At higher temperatures the fluorescence decreases further and disappears at ~120°K. Sharp lines appear at low temperatures on the low-wavelength side of the manganese emission band and are reported in more detail in Fig. 4 and Table II. A greater number of these lines were observed in the undoped sample than in the

TABLE I. Sharp absorption lines of $RbMnF_3$ at $T=19$°K.

λ (Å)	Intensity
5116	weak
5156	weak
5182	weak
5200	weak
5244	weak
5304	strong
5333	strong
5373	weak
5398	weak
5403	medium
5408	medium
5413	weak
5423	weak
5443	medium
5468	very strong
5486	medium

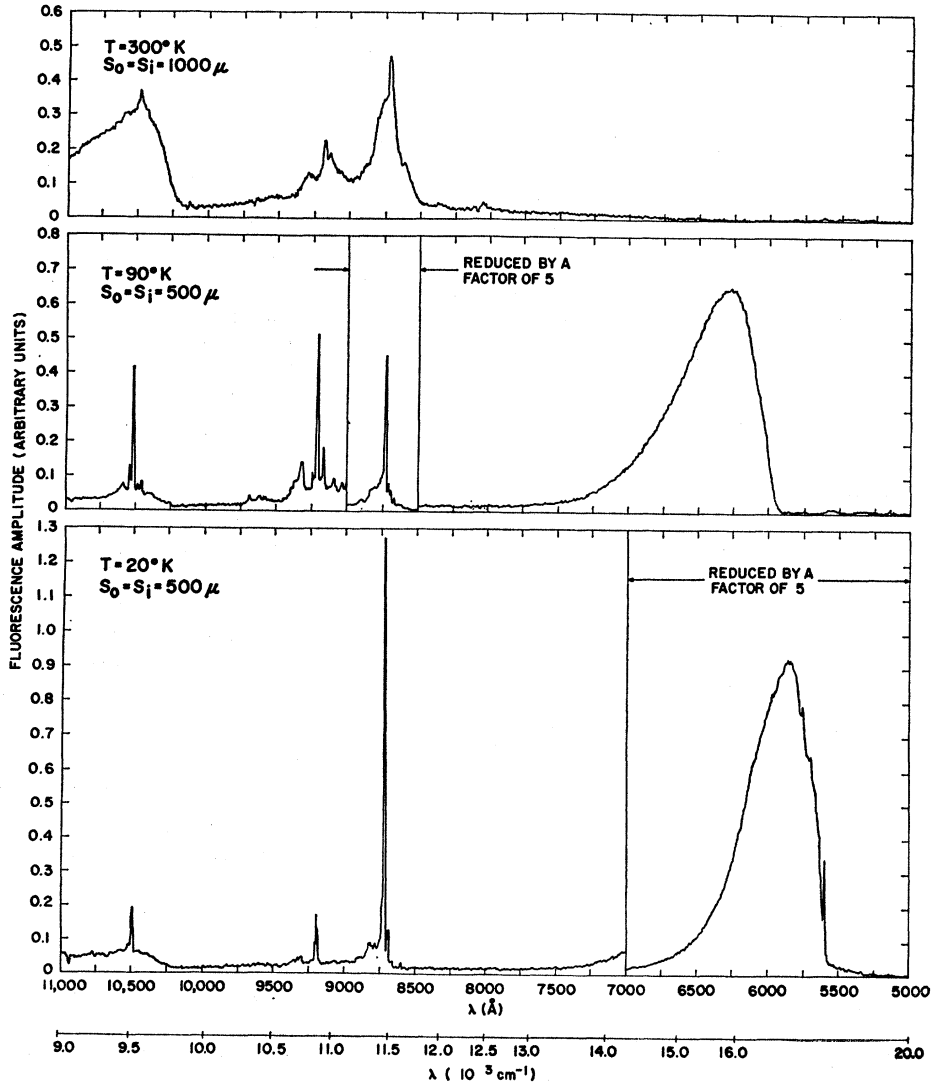

FIG. 2. Fluorescence spectra of $RbMnF_3$: Nd^{3+} (uncorrected for the S-1 photomultiplier response and for the grating efficiency; S_i and S_0 indicate the widths of the input and output slits of the monochromator, respectively).

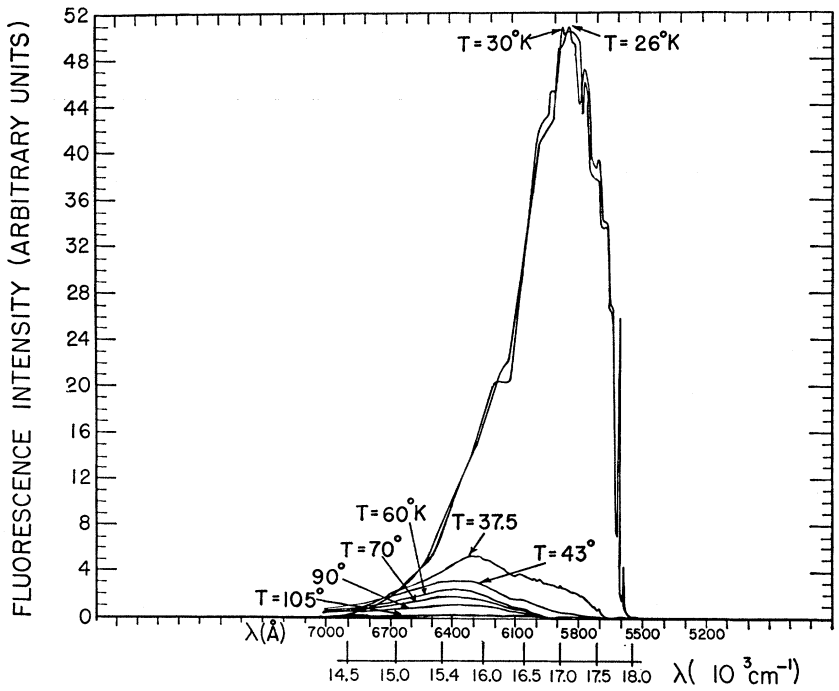

FIG. 3. Thermal dependence of the Mn^{2+} fluorescence in $RbMnF_3$.

neodymium-doped sample. They are similar to those observed in MnF_2.[8]

Figure 5 reports the excitation spectra of the Mn^{2+} fluorescence in $RbMnF_3$. These spectra were obtained by monitoring the manganese fluorescence at ~5820 Å when varying the wavelength of the pumping light through the absorption spectrum. The excitation spectra correlate very well with the absorption spectra and the bands are labeled accordingly. The same spectra (except for different intensity scales) were obtained when monitoring the Mn^{2+} fluorescence at ~6300 Å.

TABLE II. Sharp fluorescence lines of $RbMnF_3$ at $T=12°K$.

λ (Å)	Intensity
5585	medium
5592	medium
5602	strong
5612	medium
5651	weak
5665	weak
5673	medium
5705	medium
5764	medium
5956	strong
5977	strong
5990	medium
6008	weak
6022	weak
6045	weak
6093	weak
6103	weak
6118	weak
6125	strong
6143	weak
6155	weak
6170	weak

[8] R. L. Green, D. D. Sell, and R. M. White, in *Optical Properties of Ions in Crystals*, edited by H. M. Crosswhite and H. W. Moos (Interscience Publishers, New York, 1967), p. 289.

Figure 6 reports the excitation spectra of Nd^{3+} in $RbMnF_3:Nd^{3+}$. For these measurements the fluorescence was monitored by means of an interference filter centered at 1.06 μ. In the 3000–6000 Å region, most of the exciting energy corresponds to the manganese bands, giving good evidence of the $Mn^{24} \rightarrow Nd^{3+}$ energy transfer. Above 6000 Å two other bands are present due to direct excitation through the neodymium upper levels.

In order to study the effect of temperature on the $Mn \rightarrow Nd$ transfer rate, we measured the integrated intensities of the manganese and neodymium fluorescence as a function of temperature in $RbMnF_3:Nd^{3+}$. The results are reported in Fig. 7. With rise in temperature, the manganese fluorescence shows a sharp decrease at ~32°K and decreases further at ~90°K; the Nd^{3+} fluorescence increases sharply at ~32°K and then decreases slowly to a constant value at ~90°K.

B. Fluorescence Response to Pulsed Excitation

Extensive measurements of the decay pattern of the Mn^{2+} fluorescence in $RbMnF_3$ were performed. The experimental results are reported in Fig. 8. The measurements were made in the temperature region 6–120°K and at 5820 and 6300 Å, corresponding to the wavelengths of maximum fluorescence output below and above ~32°K, respectively; these wavelengths and the resolution used were such as to exclude the sharp fluorescence lines reported in Table II and Fig. 4.

The decay of the 5820 Å fluorescence is a pure exponential at all temperatures. The lifetime, as given by the time constant of this exponential, is ~55 msec up to ~25°K and then drops abruptly to reach a value of ~1 msec at 32°K. The thermal dependence of the lifetime is similar to that found by Holloway and Kestigian[9]; it differs, however, from the results of these workers in two respects: (1) at low temperature we found longer lifetimes (by a factor of about 2), and (2) the temperature at which we found the sudden change to occur was somewhat lower.

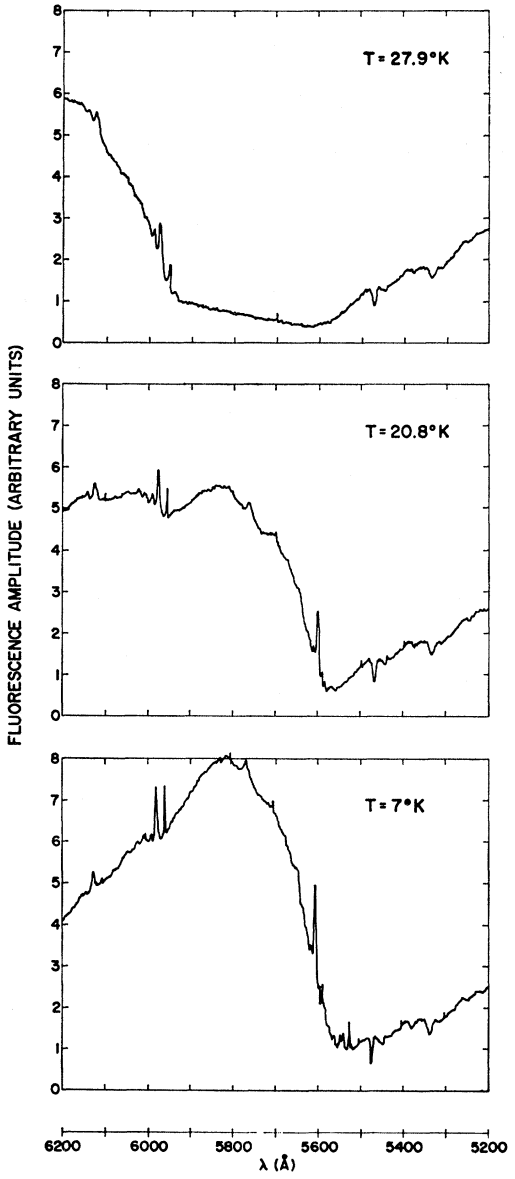

FIG. 4. Sharp fluorescence lines in $RbMnF_3$ (the dips in the scattered light above 5600 Å, correspond to absorption lines; the slits of the monochromator were set at 50 μ).

[9] W. W. Holloway and M. Kestigian, Sperry Rand Research Center, Research Report No. SRRC-RR-66-47, 1966 (unpublished).

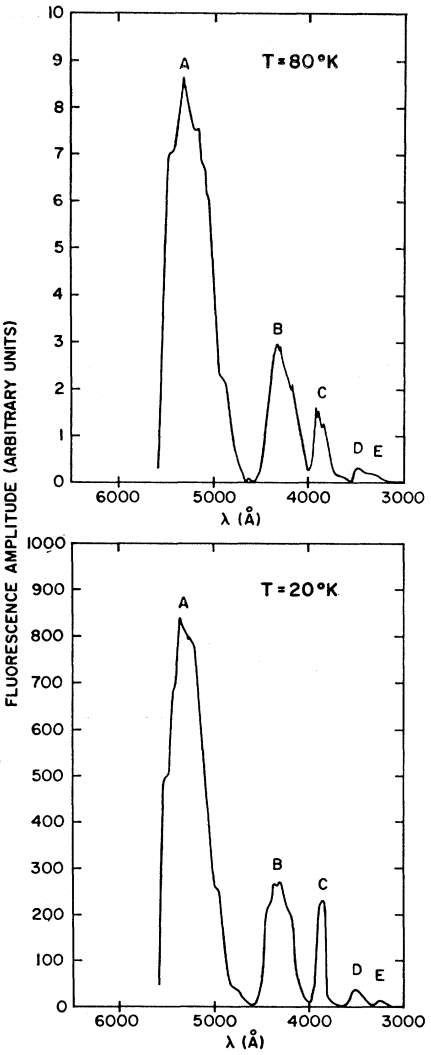

FIG. 5. Excitation spectra of Mn^{2+} in $RbMnF_3$.

The decay pattern of the 6300 Å fluorescence is rather complicated. It presents the following characteristics:

(1) At several temperatures below 40°K the decay pattern presents a rise in the fluorescence output, followed by a decay. We call t_{max} the time at which the maximum in the fluorescence signal occurs. The fluorescence rise is most noticeable in the two temperature regions 7–11°K and 25–30°K and t_{max} presents its largest values of 3 and 4 msec at 9 and 26°K, respectively.

(2) The values of the decay time of the curve following the fluorescence maximum are considered to give the intrinsic lifetime of the level from which the 6300 Å band originates. They are also reported in Fig. 8. Again, the values found here for the lifetimes at low temperature are larger (by about a factor of two) than those found by Holloway and Kestigian.[9]

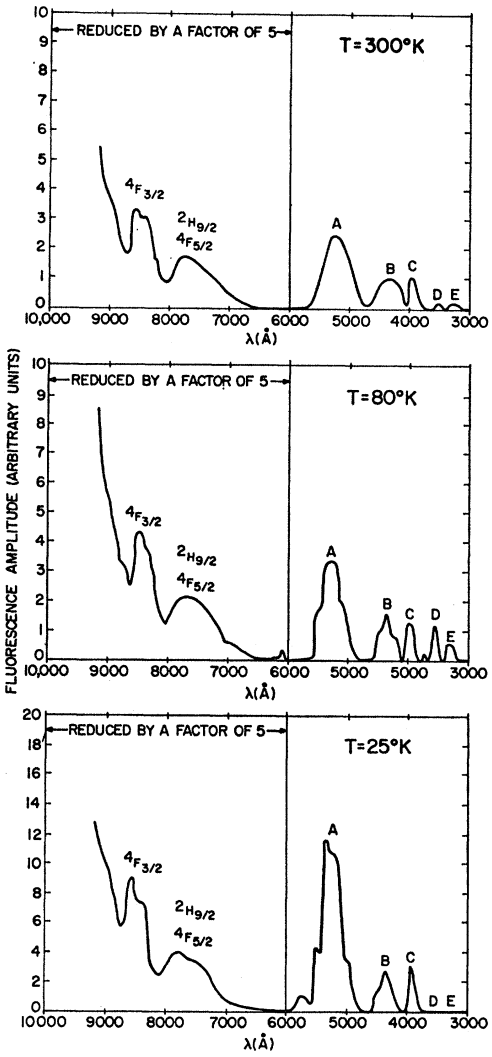

FIG. 6. Excitation spectra of Nd^{3+} in $RbMnF_3$:Nd^{3+}.

(3) The lifetime presents a value of 40 msec up to ~25°K. At this temperature a kink is observed in the curve of the lifetime which decreases suddenly to ~32 msec.

(4) From 25°K up, the lifetime decreases slowly to reach a value of ~20 msec at 85°K and then drops to ~1 msec at 110°K.

Figure 9 illustrates the behavior of the Mn^{2+} fluorescence decay at 6300 Å in the two temperature regions in which an initial rise in the signal occurs.

The fluorescence-decay characteristics of Mn^{2+} in the neodymium doped $RbMnF_3$ sample are similar to those observed in the undoped $RbMnF_3$ except that below 28°K the lifetimes at both 5820 and 6300 Å are longer in the doped than in the undoped sample by ~10 and 20 msec, respectively, and the 6300 Å band does not present an initial rise in the fluorescence signal in the 7–11°K region.

The characteristics of the Nd^{3+} decay are reported in Fig. 10. In the temperature region between 26 and 38°K the Nd^{3+} fluorescence presents an initial rise followed by a complicated decay with time constants up to ~15 msec. The time t_{max}, at which the Nd^{3+} fluorescence signal reaches its maximum value, is approximately zero up to ~26°K, increases to 1.7 msec at ~28°K and then decreases to zero at ~38°K. The decay time of the Nd^{3+} fluorescence is constant and equal to ~3 msec in the temperature regions below 22°K and above 33°K.

Figure 11 illustrates the behavior of the Nd^{3+} fluorescence decay in the temperature region in which the signal presents an initial rise.

IV. INTERPRETATION OF RESULTS

A. Thermal Dependence of Fluorescence Intensities

Considering the thermal variation of the Mn^{2+} fluorescence in Fig. 3, the observation can be made that, with temperature below ~32°K, the fluorescence does not disappear at 6300 Å; actually the emission at 5820 Å grows "on top" of the 6300 Å fluorescence. Even at very low temperatures there is evidence of a peak at 6300 Å, giving credence to the thought that, at low temperature, we have actually the superposition of two bands, rather than one single band. The fluorescence emission of Mn^{2+} can then be correlated with the energy-level diagram of Fig. 12. According to this model the absorption band A of Mn^{2+} is due to a transition from the ground state $^6A_{1g}$ to an excited state $^4T_{1g}$ and the Mn^{2+} fluorescence originates from two *real* levels centered at ~5820 Å (17 180 cm^{-1}) and 6300 Å (15 870 cm^{-1}).

The fact that the same excitation spectra are obtained regardless of the wavelength of the fluorescence monitored shows that all the Mn^{2+} ions are excited via the same absorption bands.

As indicated in Fig. 12, the Nd^{3+} fluorescence originates from the $^4F_{3/2}$ metastable level; the fluorescence lines at ~10 600 and ~8900 Å refer to the $^4F_{3/2} \rightarrow {}^4I_{11/2}$ and $^4F_{3/2} \rightarrow {}^4I_{9/2}$ transitions, respectively.

Considering the variation of the Mn^{2+} and Nd^{3+} fluorescence with temperature we can point out the following:

(1) The excitation spectra indicate that most of the Nd^{3+} pumping takes place through the Mn^{2+} bands, even at room temperature where no Mn^{2+} fluorescence is observed.

(2) The fluorescence lifetime of Nd^{3+} is ~3 msec and, except for the small temperature region 26–38°K, is independent of temperature. For this reason the variation of the Nd^{3+} intensity with temperature is attributed to the variation in the $Mn^{2+} \rightarrow Nd^{3+}$ energy transfer rate.

(3) The position and the width of the manganese fluorescence band is such that it overlaps with a Nd^{3+}

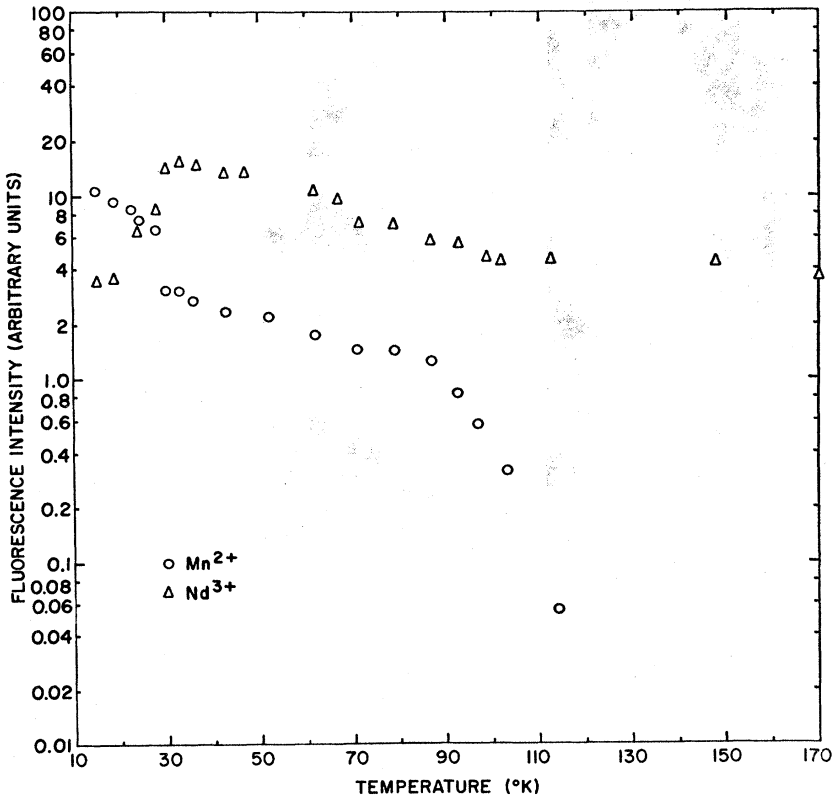

FIG. 7. Thermal dependence of the intensities of the Mn^{2+} and Nd^{3+} fluorescence in $RbMnF_3:Nd^{3+}$ (scales for the Mn^{2+} and Nd^{3+} fluorescence are unrelated).

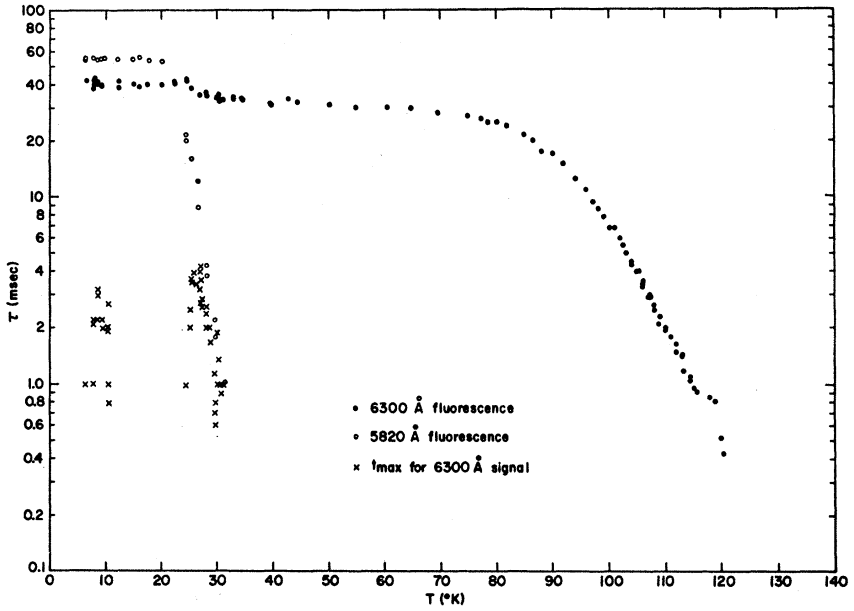

FIG. 8. The fluorescence lifetime of $RbMnF_3$ at 5820 Å and 6300 Å.

absorption band ($^2G_{7/2}$, $^4G_{5/2}$) below ~32°K. Above ~32°K the location of the manganese band does not allow for any relevant overlap. Therefore the thermal variation of the neodymium fluorescence shown in Fig. 7 is opposite to that expected on the basis of the change in the overlap of the manganese emission and the neodymium absorption.

All the points above imply that the $Mn^{2+} \rightarrow Nd^{3+}$ transfer mechanism must be of nonradiative type.

Two further observations can be made on Fig. 7:

(1) The occurrence of the sharp increase of the neodymium fluorescence at ~32°K seems to imply that the same agent is responsible for both the anomalies

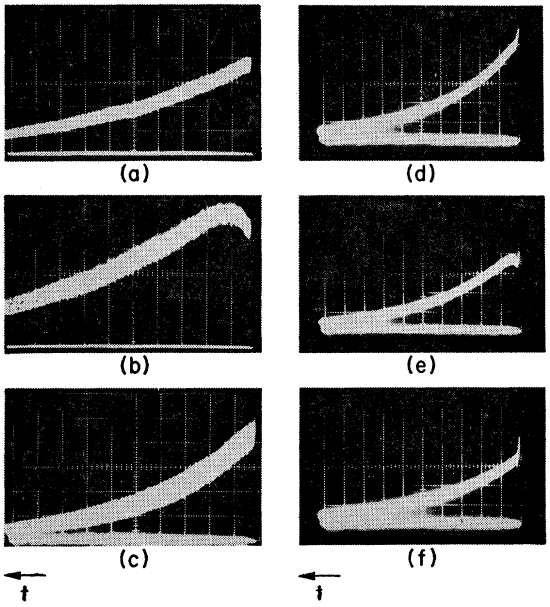

FIG. 9. Fluorescence decay of Mn^{2+} in $RbMnF_3$ at 6300 Å. (a) $T=37.9°K$; 5 msec/div; 0.2 V/cm. (b) $T=27°K$; 5 msec/div; 0.1 V/cm. (c) $T=22.4°K$; 10 msec/div; 0.1 V/cm. (d) $T=10.6°K$; 10 msec/div; 0.005 V/cm. (e) $T=10.3°K$; 10 msec/div; 0.005 V/cm. (f) $T=5.5°K$; 10 msec/div; 0.005 V/cm.

in the manganese fluorescence and the change in intensity of the neodymium fluorescence.

(2) Considering the behavior of the neodymium fluorescence at higher temperatures, we notice that the intensity tends to a constant value which it reaches at ~90°K. Since the lifetime of Nd is temperature-independent, this fact implies that no changes in the Mn → Nd transfer rate occur above this temperature.

B. Excitation and Deexcitation Processes of Mn^{2+}

The lifetime measurements provide additional information about the kinetics of the Mn^{2+} fluorescence excitation of the $Mn^{2+} \rightarrow Nd^{3+}$ energy transfer. Before examining these results consider the following theoretical arguments.

The response of two excited levels to pulsed excitation is different for the two following conditions:

(1) Fast phonon processes take place among the levels, establishing thermal equilibrium.

(2) The phonon processes among the levels are not much faster than their purely radiative decay rates. Consider now a three-level system with level one representing the ground level and levels 2 and 3 representing two excited levels. If these two levels are in thermal equilibrium, they both decay exponentially with the same lifetime given by[10]

$$\tau_F^{-1}=\frac{p_{32}p_3+p_{23}p_2}{p_{32}+p_{23}}=\frac{p_2+p_3\exp(-\Delta E_{32}/KT)}{1+\exp(-\Delta E_{32}/KT)}, \quad (1)$$

where p_{ij} represents the $i \rightarrow j$ transition probability and p_i represents the decay probability from the i level to the ground level.

If $\Delta E_{32} \gg KT$, then the lifetime is reduced to

$$\tau_F^{-1}=p_2+p_3\exp(-\Delta E_{32}/KT). \quad (2)$$

The behavior of two levels not connected by fast phonon processes may be interpreted by using the following equations for the populations of the excited states:

$$N_3(t)=N_3(0)e^{-p_3 t}$$

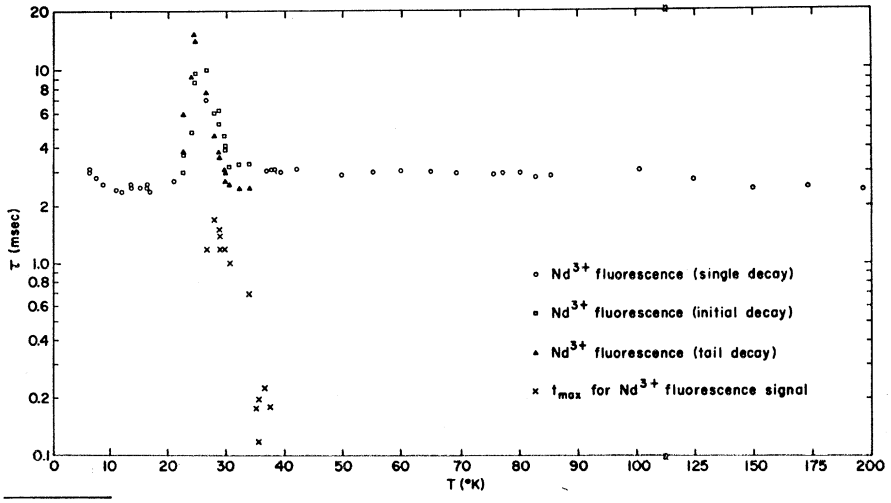

FIG. 10. Thermal dependence of the Nd^{3+} lifetime in $RbMnF_3:Nd^{3+}$.

[10] A. S. M. M. Alam and B. Di Bartolo, J. Chem. Phys. 47, 3790 (1967).

and

$$N_2(t)=\left(N_2(0)+\frac{p_{32}}{p_3-p_{21}}N_3(0)\right)e^{-p_{21}t} - \frac{p_{32}N_3(0)}{p_3-p_{21}}e^{-p_3t}, \quad (3)$$

where $t=0$ is taken at the end of the pulse, and where p_{ij} is the relaxation rate between levels i and j. Also $p_3=p_{32}+p_{31}$. If the pulse is short enough, a maximum can occur for $N_2(t)$ at a time $t_{\max}$ given by

$$t_{\max}=(p_{21}-p_3)^{-1}\ln\left(\frac{p_{21}}{p_3}+\frac{p_{21}(p_3-p_{21})}{p_3p_{32}}\frac{N_2(0)}{N_3(0)}\right). \quad (4)$$

This time is related to populations and probabilities as follows:

$$t_{\max}\geq 0 \quad \text{for} \quad p_{32}[N_3(0)/N_2(0)]\geq p_{21}. \quad (5)$$

We note that a measure of the quantity $N_2(0)$ is the amplitude of the fluorescence signal from level 2 at the end of the exciting pulse. A large value of $N_2(0)$ is evidence that the metastable level is being substantially fed *during* the exciting pulse.

Considering now the experimental results for Mn^{2+}, we observe that the different decay patterns of the Mn^{2+} fluorescence signal at ~5820 and ~6300 Å confirm the existence of two fluorescence bands; moreover, these bands must originate from two different energy levels which are *not* in thermal equilibrium.

For the 5820 Å fluorescence band we fitted the curve of the lifetime versus temperature in the whole region 5 to 35°K with a function $\tau_F(T)$ as given by Eq. (2). The fitting shown in Fig. 13 gives the rate $p_2=18.5$ sec^{-1} for the low-temperature value of τ_F^{-1}; we also find $p_3\simeq 10^9$ sec^{-1} and $\Delta E\simeq 300$ cm^{-1}. Since this difference in energy corresponds approximately to the separation in energy between the lower edge of the absorption band A and the upper edge of the fluorescence band at 5820 Å, Eq. (1) implies a thermalization condition between these two bands.[10] This condition explains also the thermal quenching of the high-energy fluorescence band as due to the redistribution of population in the metastable (5820 Å) and in the A levels, and to the very fast lifetime of level A.

We also considered the possibility of using Eq. (2) to explain the thermal quenching of the 6300 Å band above ~80°K, but we could not produce any close fitting using the data already obtained for the lifetime of the A band. This fact implies that other processes such as multiphonon decay may be active in this case.

Considering the decay pattern of the 6300 Å fluorescence, we note that most of the excitation for this band

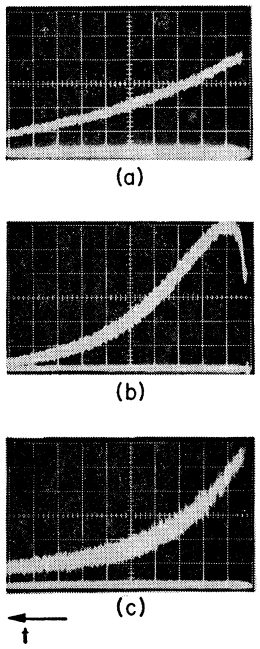

FIG. 11. Fluorescence decay of Nd^{3+} in $RbMnF_3$: (a) $T=39.1$°K; 0.5 msec/div; 0.1 V/cm. (b) $T=32.1$°K; 1 msec/div; 0.05 V/cm. (c) $T=22.4$°K; 1 msec/div; 0.02 V/cm.

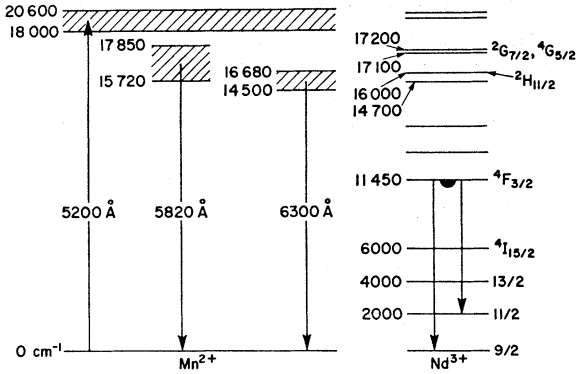

FIG. 12. Energy-level scheme for $RbMnF_3$:Nd^{3+}.

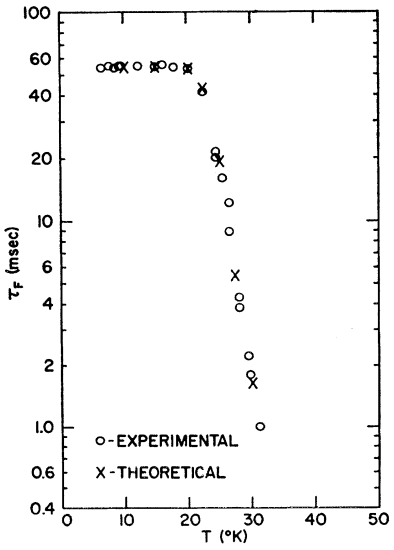

FIG. 13. Theoretical fitting of the thermal dependence of the Mn^{2+} lifetimes at ~5820 Å.

must originate from direct fast decay processes from the absorption bands. This is proved by the fact that even when presenting a rise in the fluorescence, the amplitude of the signal is large at the end of the exciting pulse and the rise produces only a *small* bump on top of a generally decaying signal. We have, however, to account for the fluorescence rise which is manifest in the 7–11 and 25–30°K regions. A possible explanation of this phenomenon is the following.

The appearance of a maximum in the fluorescence-decay signal originating from the lower level 2 of two metastable levels, 2 and 3, is controlled by the formulas (4) and (5). In particular, we note that the transfer of excitation $3 \rightarrow 2$, after the end of the pulse, depends on both the probability p_{32} and the ratio of the populations $N_3(0)/N_2(0)$. Two situations may arise:

(1) p_{32} is very small, namely, no energy transfer is taking place between levels 3 and 2;

(2) $N_3(0)$ is so small that $t_{\max}$ is not experimentally observable. Under either of these two conditions no fluorescence rise may be observed.

Referring now to the Mn^{2+} fluorescence we shall call levels 3 and 2 the metastable levels corresponding to the 5820 and to the 6300 Å bands, respectively. We shall also assume that temperature-dependent decay processes may be active between these two levels. The appearance of a maximum in the fluorescence signal is, in this model, the effect of the interplay of a probability p_{32} *increasing* with temperature and of a population $N_3(0)$ *decreasing* with temperature. This model would explain the appearance of the maximum only in the limited temperature region 25–30°K; the region below 25°K would correspond to situation (1) above, and the region above 30°K to situation (2).

A similar explanation may be given for the fluorescence rise observed for the 6300 Å band in the 7–11°K region by considering the sharp lines observed near 5600 Å (see Figs. 3 and 4). The metastable levels from which they originate have a role in this temperature region similar to that played at higher temperatures by the 5820 Å level, in that they are in thermal equilibrium with the band A and can transfer energy to the 5820 Å level through this band. Actually, the following observations can be made, on the basis of the present, non-detailed, results on these lines:

(a) Their intensity quickly decreases with increases in temperature.

(b) Their number and intensity seems to vary from sample to sample, as found by us in the two different samples examined.

(c) No rise in the 6300 Å fluorescence was observed by us in the Nd-doped sample, which, on the other hand, presented a smaller number of sharp lines.

(d) Green *et al.*[8] have examined the temperature dependence of the decay times of similar lines in the spectrum of MnF_2. The thermal variation observed by them would be consistent with the model proposed above.

C. $Mn^{2+} \rightarrow Nd^{3+}$ Energy Transfer

Let us now turn out attention to the decay pattern of the Nd^{3+} fluorescence. We can make the following observations:

(1) The Nd^{3+} intrinsic lifetime is ~ 3 msec and is essentially independent of temperature, presenting a feature generally associated with the Nd^{3+} ion in crystals.

(2) The increase in the Nd fluorescence intensity, the presence of a maximum in the decay pattern, and the lengthening of the lifetime take place in the same temperature region. This is the same temperature region where the fluorescence anomalies of Mn^{2+} are observed.

(3) All these effects in the Nd^{3+} fluorescence can be explained on the basis of a model in which the Nd^{3+} ions are excited directly from the band A. Excitation energy could proceed also from the metastable level at 5820 Å to the Nd^{3+} ions through this band. This fact could explain why both the quenching of the 5820 Å fluorescence and the increase of the Nd fluorescence take place at the same temperature.

(4) The quenching of the 5820 Å Mn^{2+} fluorescence is due to the emptying of this level into the absorption band A; when this process takes place the greater number of centers in the A band makes the $Mn \rightarrow Nd$ transfer more probable, with the consequent increase of the Nd fluorescence intensity.

(5) The lifetime data are in general consistent with this model. The presence of relevant components in the Nd^{3+} decay which produce lengthening of the apparent lifetime or a maximum in the fluorescence signal are evidence of the relevance of the process 4 above in the 25–32°K region.

It is not possible from the data reported here to draw any firm conclusions as to the nature of the two Mn^{2+} emitting states. However, there is a striking similarity in the general feature of the absorption and emission spectra of $RbMnF_3$ and those observed in molecular crystals involving free-exciton absorption and trapped-excitation emission.[11] Because of the high concentration of manganese and the relatively strong interaction between Mn^{2+} ions in $RbMnF_3$, the optical absorption may be expected to be an exciton-type process in which the excitation energy is delocalized and moves freely throughout the crystal. The movement of an exciton may be retarded by interaction with phonons or by lattice imperfections. The resulting distortion of the lattice causes a decrease in the local-exciton–energy level thus prohibiting further migration of the excitation. This trapped exciton may be thermally activated back to the free-exciton band or may lose its energy through the emission of a photon. Different fluorescence

[11] J. W. Sidman, Phys. Rev. **102**, 96 (1956).

transitions correspond to different trapping sites. This model, when applied to the experimental results for $RbMnF_3$, and $RbMnF_3$:Nd^{3+}, explains qualitatively the two emission bands of Mn^{2+}, the large decrease in energy between manganese absorption and emission, the thermal quenching of the shallower Mn^{2+} emitting center by the exciton absorption band, and the energy transfer $Mn^{2+} \rightarrow Nd^{3+}$ occuring only through the exciton absorption band.

V. SUMMARY OF RESULTS

The investigation of the absorption, excitation, and fluorescence spectra of Mn^{2+} and Nd^{3+} in $RbMnF_3$ leads to the following results:

(1) The fluorescence emission of the Mn^{2+} ion is due to two real metastable levels which can be excited only via the Mn^{2+} absorption bands.

(2) The strong thermal quenching of the intensity and lifetime of the 5820 Å bands is due to a thermalization process between the corresponding level and the short-lived A level of the lowest absorption band.

(3) The decay pattern of the 6300 Å band is explained as due to the action of fast-decay processes from the absorption band and of slower energy-transfer processes from the 5820 Å metastable level.

(4) In the Nd-doped $RbMnF_3$, the excitation spectra give evidence of $Mn \rightarrow Nd$ energy transfer even at room temperature. The $Mn^{2+} \rightarrow Nd^{3+}$energy-transfer process is of nonradiative type.

(5) The observed changes in the Nd^{3+} fluorescence intensity, decay patterns, and lifetime can be attributed to excitation of neodymium by energy transfer from the manganese-absorption bands and from the 5820 Å manganese level via the lowest Mn^{2+} absorption band.

ACKNOWLEDGMENTS

The authors wish to thank Dr. C. S. Naiman and Dr. J. Terrell for helpful discussions.

PHYSICAL REVIEW VOLUME 177, NUMBER 2 10 JANUARY 1969

Electron Paramagnetic Resonance of Gd^{3+} in Zircon Structures. II. YVO_4, YPO_4, $YAsO_4$

JACK ROSENTHAL* AND REED F. RILEY
The Bayside Laboratory, Research Center of General Telephone & Electronics Laboratories Incorporated, Bayside, New York 11360

AND

U. RANON†
McDonnell Douglas Corporation, Santa Monica, California 90406

(Received 22 August 1968)

The EPR spectrum of Gd^{3+} in the three zircon hosts YVO_4, YPO_4, and $YAsO_4$ has been analyzed and shown to fit a tetragonal spin Hamiltonian. Crystal-field parameters are given. The technique for determining the absolute sign of the axial parameters is shown.

I. INTRODUCTION

IN previous work[1] on YVO_4, hereafter referred to as I, we initiated a program of EPR investigations of Gd^{3+} in zircon structures. The present research is an extension of this program to include the two additional hosts YPO_4 and $YAsO_4$, as well as low-temperature measurements on YVO_4. As pointed out in I, most EPR investigations of S-state ions (Gd^{3+} and Eu^{2+} among the rare earths; Mn^{2+} and Fe^{3+} among the transition elements) are motivated by one (or both) of two concerns: (a) the mechanism for the removal of the ground-state spin degeneracy, and (b) the symmetry and magnitude of the host crystal field. The first is now mostly a theoretical problem because a considerable number of published spectra exist and further proliferation of results is not likely to illuminate the underlying mechanism. The emphasis will shift if any theoretical advance can suggest model systems to test theory. The second of the above concerns dominates at present, and it is our prime concern here. We hope, too, that an examination of systematics in various materials having the zircon structures will help to give some coherence to the crystal-field parameters that have been determined.

We have included a discussion of the method for determining the absolute sign of the axial crystal-field parameters.

* Present address: Dept. of Physics, New York University, New York, N. Y. 10003.

† Work presented herein was conducted by the McDonnell Douglas Corporation, Missile and Space Systems Division under Company-sponsored Independent Research and Development Program, Account No. 80271-004.

[1] J. Rosenthal, Phys. Rev. 164, 363 (1967).

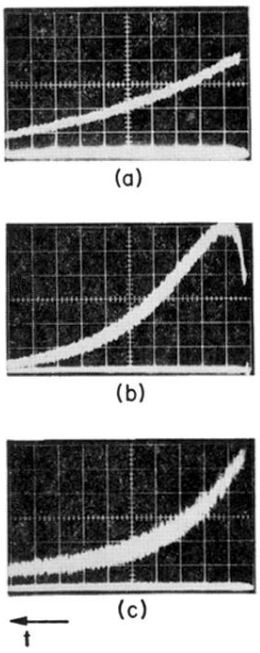

FIG. 11. Fluorescence decay of Nd^{3+} in $RbMnF_3$: (a) $T=39.1°K$; 0.5 msec/div; 0.1 V/cm. (b) $T=32.1°K$; 1 msec/div; 0.05 V/cm. (c) $T=22.4°K$; 1 msec/div; 0.02 V/cm.

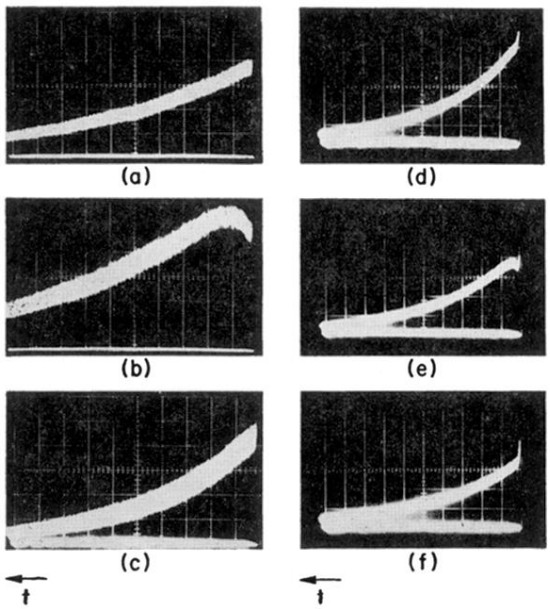

FIG. 9. Fluorescence decay of Mn^{2+} in $RbMnF_3$ at 6300 Å. (a) $T=37.9°K$; 5 msec/div; 0.2 V/cm. (b) $T=27°K$; 5 msec/div; 0.1 V/cm. (c) $T=22.4°K$; 10 msec/div; 0.1 V/cm. (d) $T=10.6°K$; 10 msec/div; 0.005 V/cm. (e) $T=10.3°K$; 10 msec/div; 0.005 V/cm. (f) $T=5.5°K$; 10 msec/div; 0.005 V/cm.